

## Effect of the Surface Curvature on the Secondary Structure of Peptides Adsorbed on Nanoparticles

Himadri S. Mandal and Heinz-Bernhard Kraatz\*

Department of Chemistry, University of Saskatchewan, 110 Science Place, Saskatoon, Canada S7N 5C9

Received January 16, 2007; E-mail: kraatz@skyway.usask.ca

In two-dimensional self-assembled monolayers (2D SAMs) on flat metal surfaces, the stability and the structure of the adsorbates depend on the interactions among neighboring molecules; for example, in alkanethiolated 2D SAMs, the adsorbates interact primarily through the intermolecular van der Waals forces and form well-packed and almost defect-free monolayers.<sup>1</sup> On the other hand, in monolayer-protected nanoparticles (3D SAMs), the interchain distance increases as one moves outward from the core and the adsorbate monolayer becomes progressively less dense, defect-prone, and irregular.<sup>2</sup> Recently, peptide-protected gold nanoparticles (GNPs) have received significant attention due to their potential relevance in biomedical applications. Demonstrations of nuclear targeting,<sup>3</sup> molecular recognition,<sup>4</sup> and protein-like properties<sup>5</sup> are truly promising. However, the secondary structure of the peptide is known to be highly dependent on the interactions with the surrounding environment,<sup>6</sup> and the effect of the curvature between crystallographic faces of GNPs (which are polyhedral species)<sup>7</sup> on the secondary structure of adsorbate peptides is still an unexplored but potentially a critical issue. In this paper, we report the structural investigation of a 16 amino acid containing peptide in both 2D and 3D SAMs (having increasing core diameters: 5, 10, and 20 nm, and thereby decreasing the curvature between crystallographic faces) on gold surfaces. We have found that the degree of surface curvature has a profound effect on the secondary structure of the peptide, and a 3D SAM (on nanoparticles) does not always resemble the 2D SAM.

The Leu-rich peptide **Ac10L** (Ac-KTAL<sub>10</sub>NPC-NH<sub>2</sub>) is a synthetic model for the  $\alpha$ -helical conformation observed in natural proteins<sup>8</sup> and possesses a thiol-functionalized Cys residue at the C-terminal (Figure 1). A preliminary account of the design, synthesis, and characterization of the peptide and preparation of both 2D and 3D SAMs are provided in the Supporting Information. We have employed<sup>9</sup> Fourier transform infrared (FT-IR) spectroscopy to probe the structure of the peptide since this technique has been one of the primary tools in understanding the secondary structure of peptides in both 2D and 3D SAMs.<sup>10</sup>

The amide I band, which is well-known for its sensitivity to the peptide secondary structure, appears at 1659 cm<sup>-1</sup> for the free peptide in KBr (Figure 2a) and indicates that the peptide is  $\alpha$ -helical.<sup>11</sup> On a flat gold surface (2D SAM), the peptide remains helical as Fourier transform reflection absorption infrared spectroscopy (FT-RAIRS) shows the amide I band at 1674 cm<sup>-1</sup> (Figure 2e). The band shifts by  $\sim 15$  cm<sup>-1</sup> compared to that in KBr, which is not related to any structural change of the  $\alpha$ -helix on the flat gold surface but rather due to the so-called optical effects.<sup>10b-d,12</sup> More specifically, this blue shift of the amide I band depends on the orientation of the helix axis relative to the gold surface; the more vertical the arrangement, the higher is the shift. Similar types of observation and interpretation were reported previously for several helical peptides in 2D SAMs on gold surfaces.<sup>10b-d</sup>

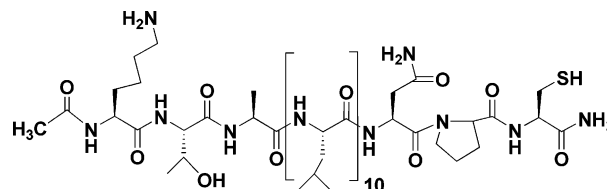


Figure 1. Molecular structure of the peptide **Ac10L**.

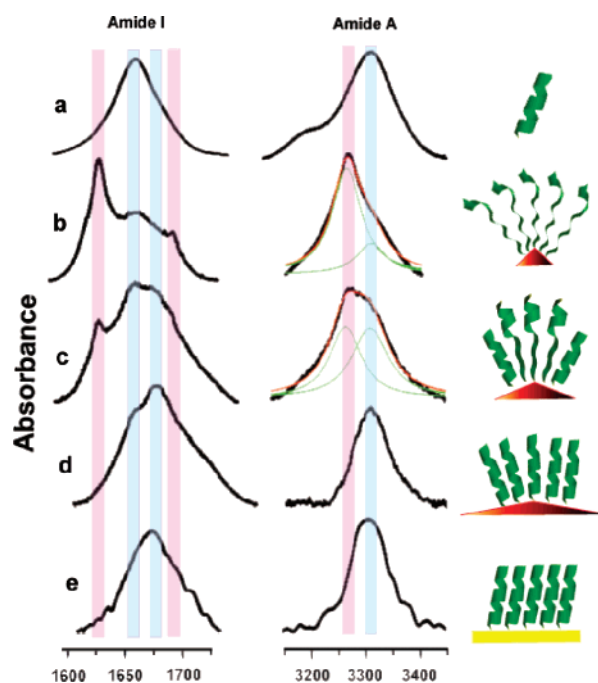


Figure 2. FT-IR spectra (KBr) of **Ac10L**: free state (a); on 5, 10, and 20 nm Au-NPCs (b, c, and d, respectively); and FT-RAIRS on flat gold surface (e). The light blue and pink shades show regions where absorptions due to  $\alpha$ - and  $\beta$ -sheet conformations occur, respectively.

Interestingly, the IR spectrum (KBr) of the peptide on 5 nm GNPs (Figure 2b) significantly differs from those of the free and 2D states. The amide I region is composed of two additional bands: an intense band at 1627 cm<sup>-1</sup> and a weak band at 1692 cm<sup>-1</sup>, which we assign to the presence of a  $\beta$ -sheet conformation of the peptide.<sup>13,14</sup> For 10 and 20 nm GNPs (Figure 2c and d, respectively), a new absorption band appears at 1675 cm<sup>-1</sup>, which is close to the amide I for the peptide on the flat gold surface and assigned to the  $\alpha$ -helices present on the flat crystallographic faces of the GNPs (shifted due to the optical effects). The band is absent in 5 nm GNPs, and the relative intensity of the band is greater in 20 nm GNPs compared to that in 10 nm, which may be correlated to a larger amount of faces in larger GNPs.<sup>7c,d</sup> In addition, by comparing the spectra of the peptide on GNPs to that of the free state, we can conclude that the absorption at 1659 cm<sup>-1</sup> (Figure

**Table 1.**  $\alpha$ -Helical and  $\beta$ -Sheet Contents of Ac10L in Free, 2D, and Different 3D SAMS from the Amide A Band

	$\alpha$ -helical content (%)	$\beta$ -sheet content (%)
free state	100	0
3D SAMS		
5 nm GNPs	22	78
10 nm GNPs	52	48
20 nm GNPs	100	0
2D SAM	100	0

2b–d) is due to the partially folded/intact helical conformation at the edges and corners of GNPs where optical effects are absent.

For 5 nm GNPs, an analogous situation is demonstrated in the amide A region (Figure 2b). Two amide A bands are observed, which implies the occurrence of two types of hydrogen-bonded N–H groups: a low-energy region (at 3266  $\text{cm}^{-1}$ ) due to the NH groups involved in  $\beta$ -sheet-like H-bonds ( $\text{C}=\text{O}\cdots\text{H}-\text{N}$ )<sup>2d,14,15</sup> and a high-energy region (at 3307  $\text{cm}^{-1}$ ) corresponding to the NH groups analogous to the native helix (intramolecular hydrogen bonds). From the deconvoluted spectrum, it can be shown that the peptide (on 5 nm GNPs) almost exclusively ( $\sim 78\%$ ) adopts  $\beta$ -sheet conformation (Table 1). In 10 nm GNPs, the relative content of the  $\beta$ -sheet is reduced ( $\sim 48\%$ ) and if the size is further increased (20 nm) it completely disappears (Figure 2b–d). The decrease in the  $\beta$ -sheet and increase in the  $\alpha$ -helical contents with the increase in the GNP size can be rationalized as follows. At the edges and corners of GNPs, the Au–S bond density has been reported to be higher compared to that in the faces because of greater unsaturation of the gold atoms.<sup>7a,b,16</sup> So the peptides bound through the Au–S bond at the edges and corners (of 5 and 10 nm GNPs) are close enough to form an intermolecular H-bond containing  $\beta$ -sheet conformation. At the periphery, where interchain distance is larger because of the surface curvature, the peptides are unable to form the intermolecular H-bonds and adopt their native structure (helix). With the increase of the size of the GNPs, the curvature of the faces and the degree of unsaturation of the gold atoms at the edges and corners reduce, which results in the decrease of the Au–S bond density and the increase in the intermolecular distance. In 20 nm GNPs, the curvature of the faces is probably negligible, and the Au–S bond density is comparable to that in the faces, and the peptides are  $\alpha$ -helical even at the edges and corners.

Our IR investigations indicate that the peptide remains helical on the flat gold surface but changes primarily to the  $\beta$ -sheet conformation on 5 nm GNPs and gradually transforms into the native helical structure as the surface curvature is reduced by increasing the size of the GNPs. This is in sharp contrast to that observed for structurally rigid unnatural amino acid Aib-containing peptides,<sup>10a</sup> in which the native secondary structure (helix) is retained even on smaller GNPs (1.1–2.3 nm). So we speculate that peptide rigidity is also very important to govern the Au–S bond density at the edges and corners of GNPs. For the natural amino acid containing peptide backbones, which are not as rigid as Aib-containing ones, the higher reactivity of the Au atoms (at edges and corners)<sup>7b</sup> dominates and forms denser Au–S bonds, whereas for structurally rigid peptides, bulkiness of the molecule controls the Au–S density.

Since the reactivity of a peptide is related to the secondary structure,<sup>17</sup> any conformational change could seriously alter the

overall activity of the peptide-protected nanoparticles, and this work may provide a somewhat cautionary note in selecting a particular peptide sequence for nanoparticle-based applications just by considering the native structure. In addition, the size of the nanoparticle should also be taken into consideration.

**Acknowledgment.** We thank the Natural Science and Engineering Research Council of Canada for funding. H.-B.K. is the Canada Research Chair in Biomaterials.

**Supporting Information Available:** Design, synthesis, and characterization details, CD and UV–vis absorption spectra, deconvoluted IR spectra with parameters, and TEM images. This material is available free of charge via the Internet at <http://pubs.acs.org>.

## References

- (1) Bain, D.; Evall, J.; Whitesides, G. M. *J. Am. Chem. Soc.* **1989**, *111*, 7155–7164.
- (2) (a) Templeton, A. C.; Hostetler, M. J.; Kraft, C. T.; Murray, R. W. *J. Am. Chem. Soc.* **1998**, *120*, 1906–1911. (b) Hostetler, M. J.; Stokes, J. J.; Murray, R. W. *Langmuir* **1996**, *12*, 3604–3612. (c) Paulini, R.; Frankamp, B. L.; Rotello, V. M. *Langmuir* **2002**, *18*, 2368–2373. (d) Boal, A. K.; Rotello, V. M. *Langmuir* **2000**, *16*, 9527–9532. (e) Weeraman, C.; Yatawara, A. K.; Bordenyuk, A. N.; Benderskii, A. V. *J. Am. Chem. Soc.* **2006**, *128*, 14244–14245.
- (3) Tkachenko, A. G.; Xie, H.; Coleman, D.; Glomm, W.; Ryan, J.; Anderson, M. F.; Franzen, S.; Feldheim, D. L. *J. Am. Chem. Soc.* **2003**, *125*, 4700–4701.
- (4) Katz, E.; Willner, I. *Angew. Chem., Int. Ed.* **2004**, *43*, 6042–6108.
- (5) Levy, R.; Thanh, N. T. K.; Doty, R. C.; Hussain, I.; Nichols, R. J.; Schiffrin, D. J.; Brust, M.; Fernig, D. G. *J. Am. Chem. Soc.* **2004**, *126*, 10076–10084.
- (6) (a) DeGrado, W. F.; Lear, J. D. *J. Am. Chem. Soc.* **1985**, *107*, 7684–7689. (b) Kiyota, T.; Lee, S.; Sugihara, G. *Biochemistry* **1996**, *35*, 13196–13204.
- (7) (a) Templeton, A. C.; Wuelfing, W. P.; Murray, R. W. *Acc. Chem. Res.* **2000**, *33*, 27–36. (b) Roduner, E. *Chem. Soc. Rev.* **2006**, *35*, 583–592. (c) Cunningham, D. A. H.; Vogel, W.; Kageyama, H.; Tsubota, S.; Haruta, M. *J. Catal.* **1998**, *177*, 1–10. (d) Gutiérrez-Wing, C.; Ascencio, J. A.; Pérez-Alvarez, M.; Marín-Almazo, M.; José-Yacamán, M. *J. Cluster Sci.* **1998**, *9*, 529–545.
- (8) Barlow, D. J.; Thornton, J. M. *J. Mol. Biol.* **1988**, *201*, 601–619.
- (9) Characterization of the 3D SAMS by CD and <sup>1</sup>H NMR was not possible due to a precipitation problem.
- (10) (a) Fabris, L.; Antonello, S.; Armelao, L.; Donkers, R. L.; Polo, F.; Toniolo, C.; Maran, F. *J. Am. Chem. Soc.* **2006**, *128*, 326–336. (b) Miura, Y.; Kimura, S.; Imanishi, Y.; Umemura, J. *Langmuir* **1999**, *15*, 1155–1160. (c) Boncheva, M.; Vogel, H. *Biophys. J.* **1997**, *73*, 1056–1072. (d) Miura, Y.; Kimura, S.; Kobayashi, S.; Iwamoto, M.; Imanishi, Y.; Umemura, J. *Chem. Phys. Lett.* **1999**, *315*, 1–6.
- (11) Kennedy, D. F.; Crisma, M.; Toniolo, C.; Chapman, D. *Biochemistry* **1991**, *30*, 6541–6548.
- (12) Allara, D. L.; Baca, A.; Pryde, C. A. *Macromolecules* **1978**, *11*, 1215–1220.
- (13) (a) Benedetti, E.; Blasio, B. D.; Pavone, V.; Pedone, C.; Toniolo, C.; Bonora, G. M. *J. Biol. Chem.* **1981**, *256*, 9229–9234. (b) Toniolo, C.; Bonora, G. M.; Showell, H.; Freer, R. J.; Becker, E. L. *Biochemistry* **1984**, *23*, 698–704. (c) Toniolo, C.; Bonora, G. M.; Pillai, V. N. R.; Mutter, M. *Macromolecules* **1980**, *13*, 772–774.
- (14) Toniolo, C.; Bonora, G. M.; Barone, V.; Bavoso, A.; Benedetti, E.; Di Blasio, B.; Grimaldi, P.; Lelj, F.; Pavone, V.; Pedone, C. *Macromolecules* **1985**, *18*, 895–902.
- (15) (a) Tam-Chang, S. W.; Biebuyck, H. A.; Whitesides, G. M.; Jeon, N.; Nuzzo, R. G. *Langmuir* **1995**, *11*, 4371–4382. (b) Clegg, R. S.; Hutchison, J. E. *Langmuir* **1996**, *12*, 5239–5243.
- (16) The higher density of the Au–S at the edges and corners of gold nanoparticles could also be partly due to the difference in the local pH and the pK constants in these particular sites compared to those in the flat crystallographic faces.
- (17) (a) Venanzi, M.; Valeri, A.; Paleschi, A.; Stella, L.; Moroder, L.; Formaggio, F.; Toniolo, C.; Pispisa, B. *Biopolymers* **2004**, *75*, 128–139. (b) Formaggio, F.; Barazza, A.; Bertocco, A.; Toniolo, C.; Broxterman, Q. B.; Kaptein, B.; Brasola, E.; Pengo, P.; Pasquato, L.; Scrimin, P. *J. Org. Chem.* **2004**, *69*, 3849–3856.

JA0703372